2022

Spontaneous Symmetry Breaking and Linear Electrooptic Response in the Achiral Ferronematic Compound

Neelam Yadav
Trinity College Dublin, Ireland

Yuri Panarin
Technological University Dublin, yuri.panarin@tudublin.ie

Wanhe Jiang
University of Hull

See next page for additional authors

Recommended Citation

Yadav, N., Panarin, Y. P., Jiang, W., Mehl, G. H., & Vij, J. K. (2022). Spontaneous Symmetry Breaking and Linear Electrooptic Response in the Achiral Ferronematic Compound. Technological University Dublin. DOI: 10.21427/MV4X-YK73

Funder: Irish Research Council

Authors
Neelam Yadav, Yuri Panarin, Wanhe Jiang, Georg H. Mehl, and J.K. Vij

Spontaneous Symmetry Breaking and Linear Electrooptic Response in the Achiral Ferronematic Compound.

Neelam Yadav[1#], Yuri P. Panarin[2#], Wanhe Jiang[3], Georg H. Mehl[3] and Jagdish K. Vij[1*]

[1]Department of Electronic and Electrical Engineering, Trinity College Dublin, The University of Dublin, Dublin 2, Ireland
[2]Department of Electrical and Electronic Engineering, TU Dublin, Dublin 7, Ireland
[3]Department of Chemistry, University of Hull, Hull HU6 7RX, UK

Abstract: A compound with the constituent non-chiral molecules, DIO, known to exhibit three nematic subphases namely N, Nx and N_F, is studied by polarizing microscopy as function of the alignment layers on one of the substrates, no alignment on any of the substrates, alignment layer on both substrates with parallel and antiparallel rubbing, different cell spacings. The cell with one alignment layer is also studied by electro-optics. N is found to be a conventional nematic phase, but it shows two additional unusual features: chiral domains of opposite chirality and the linear EO response to the applied signal under certain experimental conditions. The emergence of chiral domains is explained by a segregation of the stable helical conformers of the opposite chirality, these preferring to form chiral domains, each with optical rotation power of ± 4°/μm. This is the first example of helical segregation observed in non-chiral molecules in the high temperature nematic phase. The conformers are suggested to arise from the rotations of the aromatic rings either left-handed or right-handed. Unlike the ordinary nematic liquid crystalline phase, linear electrooptical response to the applied electric field (i. e. to its fundamental frequency) is observed, this confirms the polar nature of this phase. The N_F is the ferroelectric nematic as reported previously. The strong polar azimuthal surface interaction energy in N_F phase stabilizes a homogeneous structure in planar aligned LC cells rubbed parallel and in cell rubbed antiparallel, it gives a twisted structure. The transmission spectra simulated using Berreman's 4 x 4 matrix method for different cell conditions and for different angles between the Polarizer and the Analyzer quantitatively confirm the twisted structures in antiparallel rubbed cells that agree with experimental observations. The twist angle of 170° is found between the directors from the top to the bottom in antiparallel rubbed cells as opposed to 180° observed previously.

joint first authors
*jvij@tcd.ie

1. Introduction

Despite predictions for the existence of ferroelectric nematic phase (N_F) made over a century ago by Born [1], this phase has only been recently discovered in a limited number of chemical systems: two nematic phases in RM 734-series [2], three nematic subphases in DIO [3] and in a highly fluorinated rigid mesogens with similar molecular structure to DIO but without the ester group being present [4]. In these systems, the conventional nematic phase is observed at higher temperatures while the N_F phase is observed at lower temperatures. This three-dimensional liquid crystalline compound displays spontaneous polar ordering with extremely large order parameter (≥ 0.9) and it also exhibits an extremely large spontaneous polarization (~5 μC/cm^2) [2,3,5]. To form the ferroelectric state in the nematic phase, the dipole moments in these materials, μ should be as large as ~10 D, such that the interactions withstand the thermal fluctuations [6], that tentatively satisfy the equation, $\frac{\mu^2}{\varepsilon_0 \varepsilon V} > k_B T$, where V is the molecular volume, k_B is the T is the thermal energy. The pre-requisites for the formation of ferroelectric nematic phase are that the constituent molecules should have large dipole moment and a specific relative arrangement of neighboring molecular dipoles. This has recently been theoretically confirmed by Madhusudana [7]. The other recently proposed theoretical models suggest the importance of including the flexo-dipolar terms in the Landau energy expansion. These are found to play important role in providing stability to the ferroelectric nematic phase [8,9,10] with different splay deformations. However, the fluorinated N_F materials [3,4] do not show splay deformations and in these cases, ferroelectricity in a ferroelectric nematic phase may be of different origin than of the splay nematic. Therefore, the N_F phase needs further investigations using a range of complementary physical techniques to clarify the structure – property relationship. Furthermore, the mechanism for the nematic-nematic transitions and the structural characteristics of the new nematic phases needs investigations in greater detail.

This material exhibits three different nematic phases: nematic (N), intermediate nematic (N_X) and the ferroelectric (N_F) phases. Work presented in this paper is focused on studying the high temperature nematic phase of DIO not attempted, to our knowledge, in the literature so far. Chiral domains of opposite handedness are observed under sample confinement conditions arising presumably from chiral symmetry breaking. Furthermore, we investigate the response of a planar aligned cell, in the high temperature nematic phase, to the sinusoidal signal applied at a frequency in the range 10 Hz to 10 kHz both for the

fundamental and its second harmonic frequency. In this experiment, a finite response is observed at the fundamental frequency of the applied signal in a conventional paraelectric nematic phase. In addition, we investigate texture in a planar antiparallel rubbed cell and based on the comparison of experimental results with those of the simulations, a twisted structure of the directors is observed from the bottom to the top substrates. These quantitative results being reported in the N_F phase reveal differences to those already reported in the literature. In this experiment, a finite response is observed at the fundamental frequency of the applied signal in contrast to the observations of the response at the second harmonic frequency from a conventional paraelectric nematic phase. In addition, we investigate texture in a planar antiparallel rubbed cell by drawing a comparison of the experimental results with those of the simulations.

2. Results and Discussion:

Structure of the compound DIO and its phase transition temperatures are given in Figure 1. The phase sequence is confirmed as Iso - N– Nx - N_F by differential scanning calorimetry (DSC); Iso refers to the isotropic state, N to the ordinary nematic phase, N_X to an unknown nematic and N_F is a ferroelectric nematic phase. N_X is characterized as having a modulated structure at the nanoscale level and is found to be smectic-like SmZ_A antiferroelectric [11].

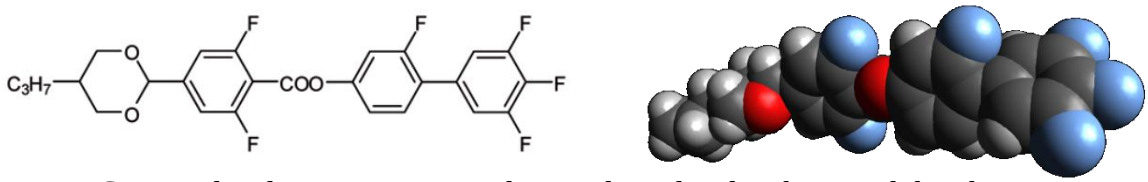

FIG. 1. Molecular structure, Van der Waals molecular shape and the phase sequence of DIO.

This compound was first synthesized by Nishikawa et. al [3]. For the works reported here, DIO is resynthesized by the group of G. H. Mehl at the University of Hull, Hull, UK.

2.1. Observation of the Chiral domains in the high temperature N phase

The textural studies using POM are extremely useful for determining the characteristics of the LC phases. The textures of DIO were studied in Ref. [3,11,12,13] in thin planar and homeotropic aligned cells. In the present study, commercial planar cells of varying thicknesses viz. 2-25 μm designed by E.H.C. Co. Ltd. were used unless otherwise specified. Texture of the ferronematic phase (including DIO and compounds of RM734-series) were found to be strongly dependent on the surface treatments, temperature/phase

and the cell thickness due to the strong interaction between the large molecular dipole moment and the surfaces [5,14]. This raises an interesting question – what textures will be realized in the bulk? To address this, we perform the optical study of a specially prepared 5 μm cell with only one rubbed surface. This cell was prepared by sandwiching two ITO coated glass substrates, out of which only one of them was coated with RN1175 (Nissan Chemicals) and subsequently rubbed after keeping it at a temperature of 250°C for one hour in the oven while the other substrate was uncoated and unrubbed. In such a case of one-surface rubbed cell, the molecular director at this surface is anchored along the rubbing direction, while the director on the opposite second surface is free to rotate. In this case, the texture should show the natural structure of that of bulk.

The textures were recorded on cooling from the isotropic state down to the N_F phase via N and N_X subphases. In a conventional N phase, the textures of one rubbed surface cells are expected to be homogeneously planar, however these show two opposite optically active areas/domains in the cell, shown in Figure 2. By rotating the analyzer by an angle of +20° (clockwise), one domain in Fig. 2b appears dark. The reverse is true for the second domain (not shown in the Figure), it shows extinction by an anticlockwise rotation (opposite rotation) of the analyzer by an angle of -20°. This means that domains of the opposite chirality do exist even in the high temperature ordinary (paraelectric) nematic phase that emerges just below the Iso-N phase transition temperature when at least one of the two planar alignment surfaces of the cell is unrubbed. Hence, this natural texture represents a conglomerate of stochastically distributed chiral areas/domains with the experimentally determined optical activity, with the rotation power of ~4 degrees/μm. In a usual two rubbed surface cells, optically active texture is affected by both surfaces. These suppress the natural optical activity, and the textures are usually homogeneously planar.

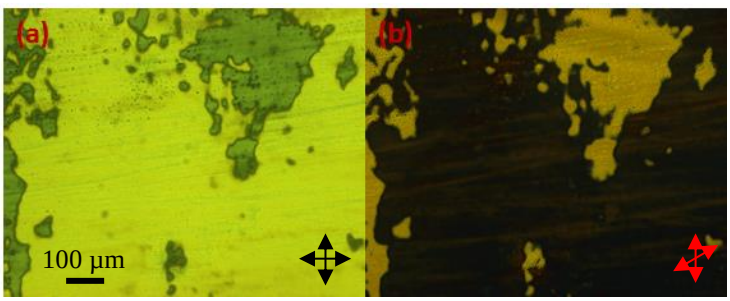

FIG. 2: Snapshots of a 5 μm thick cell at a temperature of 170 °C in the nematic phase; one of the glass plates in the cell is rubbed for homogeneous planar alignment while the second plate is unrubbed and uncoated ITO; (a) crossed polarizers (b) the analyzer is rotated clockwise by 20°.

Similar chiral domains are visible in a cell made from two unrubbed, but polymer coated ITO plates with thickness of 8 µm (refer fig. 3). To further confirm our results, cells are made with untreated ITO glass plates as well, surprisingly, this cell also shows chiral domains of opposite chirality (refer fig. 4). Chiral textures involving non-chiral molecular systems have been reported before in different phases, such as: the bent-core (BC) smectic LCs [15,16]; twist-bent nematics, (N_{TB}) [17,18] and even in some isotropic liquids [19]. The symmetry breaking in the first two systems is caused by a strong non-calamitic shape of the bent molecular core or dimers, which most likely is not the case for DIO. In DIO, chirality of domains arises from symmetry breaking like in the isotropic liquids [19]. It is pertinent to mention that this observation of chiral domains in the high temperature N phase of ferronematic liquid crystals is for the first time.

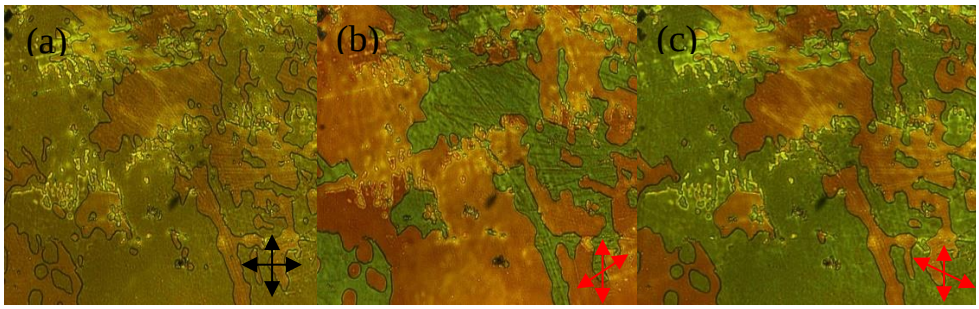

Fig. 3. The textures of 8 µm, unrubbed (both surfaces) cell for different polarizer configurations at a temperature of 160 ^{o}C in the nematic phase.

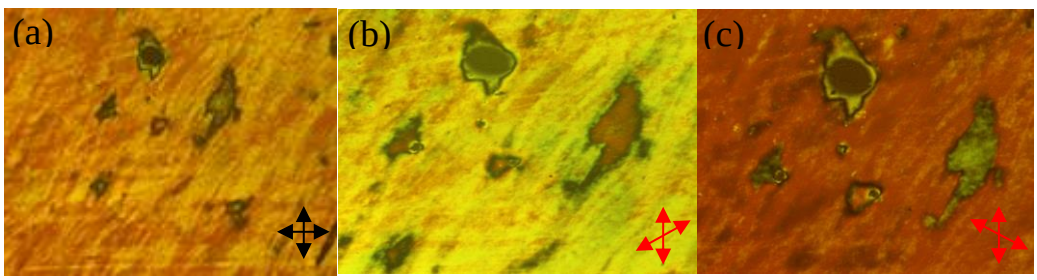

Fig 4. Textures of 6 µm cell made from two uncoated and unrubbed ITO glass plates for different polarizer positions at 160 ^{o}C in the nematic phase.

The preferred features of the system DIO are: (i) large net molecular dipole moment; (ii) the long molecular core consisting of three or more aromatic rings. The aromatic rings in these molecules have two stable states twisted at some angle between the two neighboring rings which can be positive for clockwise (or Right, R) or negative for anticlockwise (or Left, L) rotations. In the case of a compound having three or more aromatic rings, the rings may twist either in the left or the right direction forming LL…and RR… respectively or rotate in the opposite direction consecutively to form non-chiral non-helical conformers

LR…/RL. The molecular modeling software Gaussian 09 gives global minimum energy levels lie at E=192.884 Units for helical conformers and local minimum of E=192.961 units for non-helical conformers.

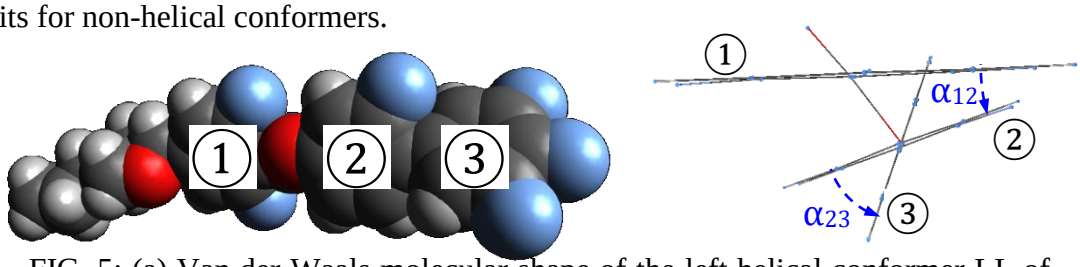

FIG. 5: (a) Van der Waals molecular shape of the left helical conformer LL of DIO and (b) side view on the aromatic rings 1-3. Rotation angles $\alpha_{12} \cong -20^{o}$ and $\alpha_{23} \cong -48^{o}$.

This implies that helical conformers of DIO (LL/RR) are more thermodynamically stable than the non-helical conformers (LR/RL). A left-handed helical conformer LL is shown in Figure 5(a), where three principal rings are numbered as 1-3. Figure 5(b) shows the side view of the angular orientations of these three rings with angles of rotation $\alpha_{12} \cong - 20^{o}$ and $\alpha_{23} \cong - 48^{o}$ between them. Possible reasons may include conformers of the same chirality having denser molecular packing, leading to a lower potential energy for the homochiral domains and hence the gain achieved in the strength of chiral discrimination ($-\Delta H_{cd}$) exceeds entropic penalty of the de-mixing process ($T \cdot \Delta S$) [19,20]. Furthermore, this twisted organization in the domains/clusters is likely to contribute to chiral segregation of helical molecular conformers as these could stabilize helical conformations by a co-operative coupling between the molecular and the nano structural twist sense, thus increasing the energy gain of homochiral packing. Based on our observations, we conclude that compound DIO under investigation in the ordinary conventional nematic phase, shows chiral domains of the opposite chirality arising from a chiral segregation of helical molecular conformers of opposite symmetry. These chiral domains may be suppressed by surface interactions as in previous studies [3,5,10]. Also, to test whether molecular structure and surface anchoring plays a role in forming these structures in DIO, similar kind of cells are filled with the ubiquitous nematic 5CB and no chiral domains are observed (refer Fig. 6). This result further confirms our conclusion.

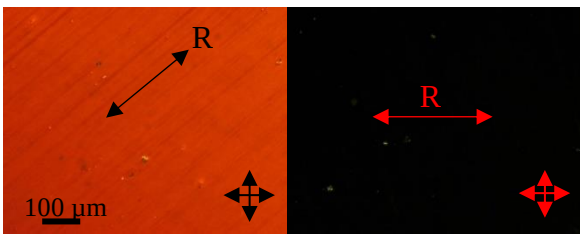

Fig. 6. The texture of classic Nematic LC 5CB filled in only 1-rubbed cell with a cell thickness of 7 μm recorded at 32 °C.

2.2 Field induced chiral domain in the high temperature Nematic phase

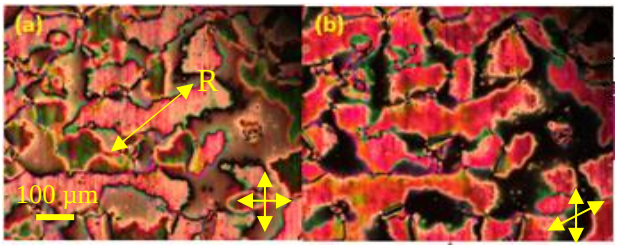

FIG. 7. Textures observed in the N phase (5 V applied across a thick cell (15 μm)) at T=150 °C with antiparallel buffed planar alignment layers (a) the image is recorded under crossed polarizers and (b) for uncrossed polarizer and analyzer by +12°.

Furthermore, in cells with both ITO surfaces coated and rubbed antiparallel, a homogeneously planar texture is stabilized initially in the N phase. At the Iso-N phase transition temperature, homogeneously uniform structure in these antiparallel rubbed cells is due to the quadrupolar term (W_Q) in the azimuthal anchoring energy (see Eq.5 in Ref. [14]) energy and this quasi-stable structure is retained in the entire temperature range of the N phase. However, on the application of an electric field greater than 0.3 V/μm perpendicular to the ITO electrodes in the N phase, the POM images show emergence of the two sets of chiral polar domains (Fig. 7). Once formed, these domains continue to exist even after the electric field is removed. Uncrossing the polarizers by an angle +12° in a specific direction darkens one set of domains and brightens the other, as seen in Fig.7b. The opposite is observed for rotation in the opposite direction-12° (not shown in Figure 7). The rotation of the hot stage mounted on the rotational stage however does not affect the relative brightness of these domains. This shows that the domains are chiral and are of opposite chirality with the polarization of light rotated as ~ 1 degree/μm, by each domain. The value is lower than of the natural rotation power (~4 degrees/μm) achieved for one-sided rubbed cell (Fig. 2). The difference in the rotation powers in these two cases can be explained by the quadrupolar term (W_Q) in the azimuthal anchoring energy (see Eq.5 Ref. [14]) which tends to suppress or reduce the natural optical rotation power.

2.3. Electro-optical dynamics in the high temperature N phase

Results obtained from the POM show polarity and chirality of the domains in the high-temperature nematic phase. The domains display a strong dependence on the cell thickness, surface treatment and temperature/phase of the sample. To investigate a

development of the polar order with temperature, we performed electro-optical (EO) measurements in planar-aligned cells. The electric field of varying voltages (0.1 V - 10 V) at frequencies (6 Hz - 100 kHz) with a sine-wave dependence of voltage on time was applied across the LC cell placed between the crossed polarizers such that the angle between the rubbing direction, and the polarizer/analyzer axis, is 45° [21]. The output signal from the photodetector was fed to the input of a DSP lock-in amplifier (SR830) and the intensity of the transmitted light through the cell was recorded for the first and the second harmonics of the applied signal.

A change in the transmittance through the cell is exclusively dependent on a change in the macroscopic refractive index Δn_{eff}. The effective birefringence is dependent on the angle θ between the LC director and the electric field as:

$$\Delta n_{eff} = \frac{n_o n_e}{\sqrt{n_e^2 \cdot \cos^2(\theta) + n_o^2 \cdot \sin^2(\theta)}} - n_o \qquad (1).$$

The average director in the absence of the field is parallel to the substrate's plane (for E = 0, θ = 90°, $\Delta n_{eff} = \Delta n = n_e - n_o$). On the application of the electric field, the director twists away the plane of the surfaces. This results into a splay deformation (the so-called S-effect) reducing effective birefringence Δn_{eff} as θ < 90^0. For a sufficiently high applied voltage to the cell the polar angle θ → 0°, $\Delta n_{eff} \to 0$ and the texture becomes almost homeotropic with a negligible light transmittance occurring in the experiment.

For a conventional paraelectric nematic phase, the output of electro-optical signal is only of the second harmonic and is strongly dependent on the frequency of the applied field. For frequencies much lower than the relaxation frequency of the LC structure, the electro-optic response gives maximal signal for the second harmonic. For frequencies much higher than LC relaxation frequency, the electrooptic response is small. For intermediate frequencies, the second-harmonic electrooptic response decreases with an increase in the frequency as the 1st order low-pass filter with a slope of -20 dB/decade. This scenario is observed in the higher temperature range of N nematic, i. e., for T ≥ 150 ^{o}C. However, the polarity and the chirality exist even in the paraelectric N nematic phase at lower temperatures. Therefore, one may expect the first harmonic response to appear arising from the polar interactions with the electric field. Figure 8a shows the frequency dependence of the magnitude ($R \cdot exp(j\theta) = X+jY$) of both the first and the second harmonics for applied

sinusoidal signal of amplitude 5 V, for three temperatures below the benchmark temperature of 150 ºC. These are set at 140 ºC, 130 ºC and 110 ºC. these temperatures correspond to the higher temperature nematic phase of DIO. However, the characteristics of the EO response are different for these three temperatures. For 140 ºC, there is a finite but a lower output of the first harmonic than of the second. The spectra for first and second harmonics show two slopes: -20 dB/decade in the low frequency range and the -40 dB/decade in the high frequency range. At a mid-temperature in the nematic phase (130 ºC) the response is similar, but the level of noise signal is higher, especially for the 1st harmonic. At the lowest temperature of 110 ºC, the spectra are not regular but are observed to be extremely noisy. To elucidate this feature, we plot the dependence of the real part *X* of the signal *R* on time in Fig. 8b of the EO response for a fixed frequency (28 Hz), measured at an interval of one minute.

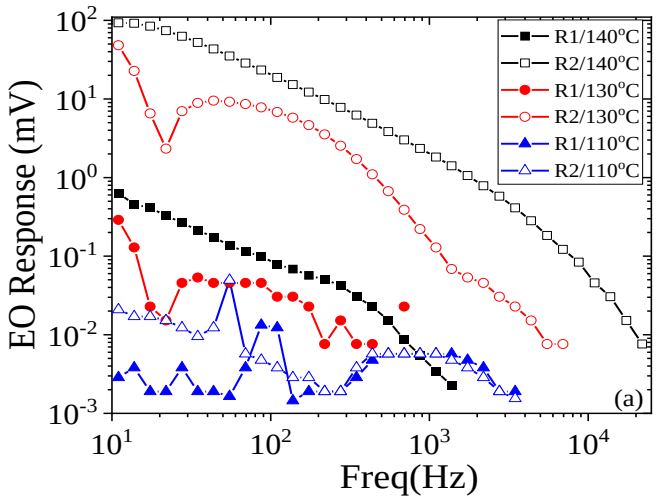

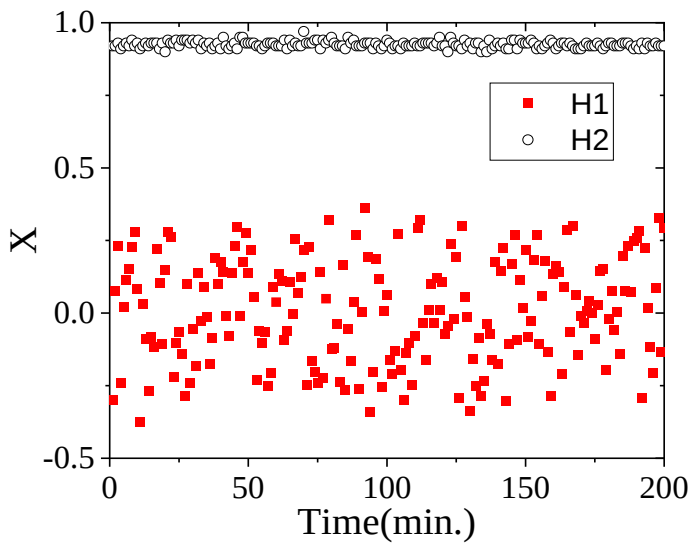

FIG. 8: (a) Frequency dependence of the magnitude (R) of the EO response of 1st harmonic (filled symbols) R1 and the 2nd harmonic (open symbols) for 5 V applied voltage at three temperatures of 110°C, 130 °C and 140°C. These temperatures of the material correspond to the conventional N phase of DIO. (b) The real part (X) of the 1st (■) [H1] and the 2nd harmonic [H2] (○), of EO response at a temperature of 110 °C are plotted as a function of time for a fixed frequency of 28 Hz, 5 V voltage signal applied. In each case, the data is recorded at a time interval of 1 min.

Both the magnitude and the phase part of the 2nd harmonic signal is stable with time while the 1st harmonic output shows no regularity with time and the output is noisy. Out of the 200 data points shown in Fig. 8b, magnitude of the signal varies roughly from –40 µV to +40 µV. The observation of the first harmonic signal R1 is not as dominant as from the twist bend structure found before, in that case the signal was obtained from a single chiral domain [18] unlike here. This observed phenomenon has a rather simple explanation. The texture of the planar-aligned antiparallel rubbed cell (Fig.7) arises from two chiral domains of the opposite polarity. The space ratio of these domain is not exactly 1:1, as seen from Fig.7b where the total area of the right domains (appearing dark under uncrossed polarizers) is less than of the left-handed domains. Moreover, this changes after each state of ON/OFF applied signal. The right-handed domains produce positive response whereas the left-handed domains lead to the opposite response. Therefore, the real part of the magnitude and the sign of response is proportional to the enantiomer excess, defined as $R = \frac{A_R - A_L}{A_R + A_L}$, changes in which are irregular with time. The 2nd harmonic response is driven by the non-polar interaction $\Delta\varepsilon \cdot E^2$ and it is regular and stable with time.

2.4 Optical Textures and birefringence measurements of the three Nematic phases in Planar-aligned cells

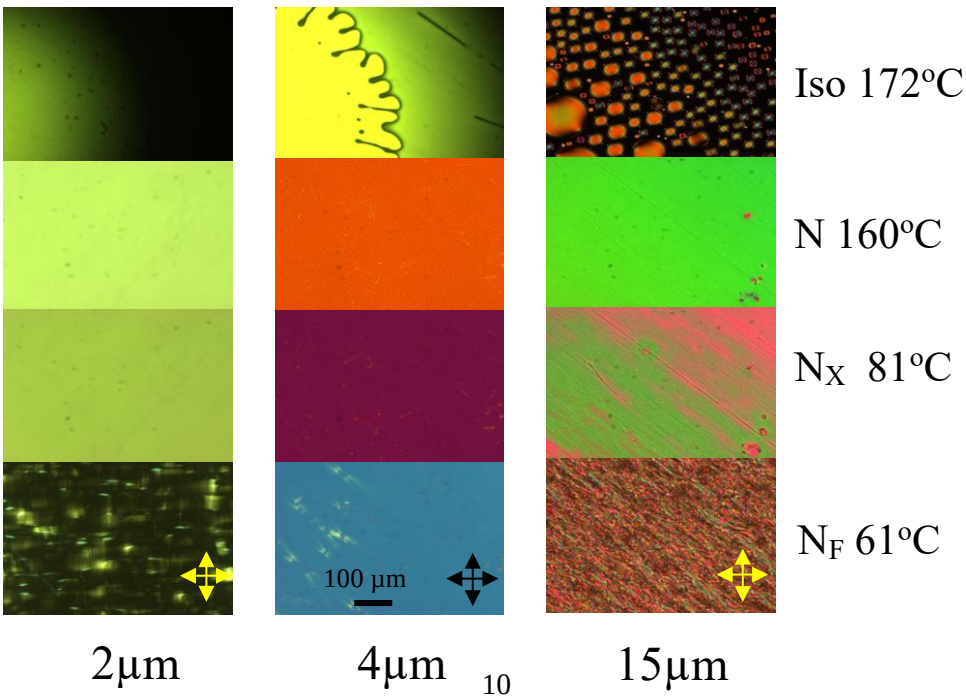

FIG. 9 Textures for different temperatures/phases recorded from planar-aligned cells of different cell thickness with unidirectional antiparallel buffed alignment on opposite surfaces.

Figure 9 displays the textures of planar-aligned cells of different thicknesses with two surfaces rubbed antiparallel. The LC cell is mounted on the rotational stage of the polarizing optical microscope (POM), with polarizer and analyzer crossed. In these experiments, the rubbing direction makes an angle ψ=45° with the axis of the polarizer in each of the cells. Homogeneous and uniform textures are observed in the three cells as the temperature is lowered from the Iso state. A change in the color of the texture depends on the optical retardation $(\pi \cdot \Delta n \cdot d)/\lambda$ experience by the light, this is dependent on the cell thickness, birefringence, and the wavelength of light (see Fig. 9). The birefringence is observed to gradually grow under cooling from the Iso state, the increase in the N-phase is caused by an increase in the order parameter.

In the two nematic phases: N and N_X, the textures are observed typically homogeneous with the optical axis/director lying along the rubbing direction in thin cells. However, in a thick (15 μm) cell, at a temperature in the N_X phase (81 ^{o}C), the texture though homogeneously uniform but some red colored domains of higher birefringence are superimposed on the green texture. The size of the red colored domains grows under cooling. In the N_F phase however, a few yellow-colored domains are also observed even in thinner cells, and these are found chiral in nature. The total area of the chiral domains grows continuously under cooling. In a thick (15 μm) cell, the texture shows many ferroelectric domains, the emergence of these domains is sensitive to the alignment layer/s and the surface treatment of substrates [12].

The birefringence measurements are based on measuring the transmittance spectra of a homogenous aligned 25 μm thick cell. Experimentally, the transmittance spectra from a planar-aligned cell for different temperatures are recorded using achromatic source of light, the spectral content of which contains an entire range of the visible wavelengths. In such a homogeneous cell, the transmittance T is given by

$$T = A \cdot \sin^2\left(\frac{\pi \cdot \Delta n_{eff} \cdot d}{\lambda}\right) + B \qquad (2)$$

In Eqn. (2) A is the scaling factor, B is the leakage of light through the cell, d is the cell thickness and Δn_{eff} is the effective birefringence, dependent on the out-of-plane angle θ and

on the dispersion of the birefringence with the wavelength of light. The latter dependence is governed by an extended Cauchy equation [Eqn. (3)] as:

$$\Delta n(\lambda) = k \cdot \frac{\lambda^2 \lambda^{*2}}{\lambda^2 - \lambda^{*2}}, \qquad (3).$$

Here k is proportional to the order parameter Q dependent on temperature and λ^* is the temperature independent dispersion parameter. The transmittance (T) spectra were measured using Avantes AvaSpec-2048 fiber spectrometer from a temperature of 171 ^oC (just below the isotropic to nematic transition temperature) down to 40 ^oC, with a temperature step of 1^oC. The experimental data are fitted to Eqn. (1), on considering dependence of Δn on the wavelength given by Eqn. (2). λ^* is deduced as 208 nm from a fitting of the T at 171 ^oC (just below the I-N transition temperature). The value of λ^* found is fixed for other temperatures. Figure 10 shows the dependence of birefringence on temperature for λ = 550 nm, the dispersion of the refractive index on wavelength at 90 ^oC in the high temperature nematic phase is given in the inset of Fig. 10. Results of the birefringence are found to be in good agreement with the previously obtained results on this compound [10,13].

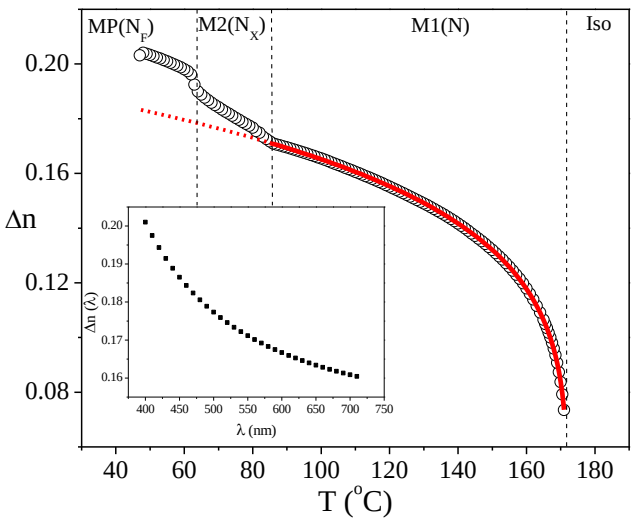

FIG. 10. The birefringence (Δn) measured for λ = 550 nm is plotted as a function of temperature for a homogeneous 25 µm thick cell. The inset shows a plot of the dispersion of birefringence with wavelength of light at a temperature of 90 ^oC.

The highest value of the birefringence in the N phase is 0.166, for which the texture of 15 µm cell looks green. The birefringence, just below N_X -N_F phase transition, temperature, jumps to 0.195 where it looks red in POM. On cooling the sample to the temperature of

the intermediate N_X phase, the higher-birefringence (red) domains appear on the low-birefringence (green) field, size of these domains grows on cooling. In the temperature range lying in the middle of the N_X phase (81°), the texture comprises almost 50% / 50% of the high- and the low-birefringence domains, and finally higher birefringence domains occupy the entire area of the cell at the transition to the N_F phase, while birefringence grows almost linearly cross the N_X phase as an average of the high- and low-birefringence areas. This may suggest that intermediate N_X phase though thermodynamically stable (following results of the DSC studies [3]) may have a possibility of the phase being a mixture of the N and N_F domains under some experimental conditions, nevertheless the quantitative studies do show that it is an antiferroelectric phase. This needs to be examined in greater detail in future. However, we also note that structures/textures are very sensitive to the cell parameters, as in ref [11] N_X phase has a modulated, so-called SmZ_A structure or it is a splay modulated phase as in ref. [pre review] If the high-temperature N phase is ordinary nematic, the temperature dependence of the birefringence should follow the Haller equation [22]:

$$\Delta n(T) = \Delta n_0 \cdot Q = \Delta n_0 \cdot \left(1 - \frac{T}{T_{IN}}\right)^{\beta} \qquad (4).$$

Here Δn_0 is the maximum birefringence reached for order parameter Q = 1, T_{IN} is Iso-N phase transition temperature and the exponent β = 0.2 ± 0.03 is obtained from a fitting of the data to Eqn. (4). Fitting of $\Delta n(T)$ to Eqn. (4) with the exponent β shows a perfect match to the experimental data (see the red line, Fig. 10) with the parameters: Δn_0=0.18; β=0.18 and T_{NI}=172 °C. An excellent fitting of the data to Eqn. (4) confirms that N behaves like a conventional nematic phase under the specified surface conditions. In addition, the N phase exhibits additional features: (a) existence of the chiral domains with the opposite chirality and (b) observation of the linear EO response, discussed already in section 2.3.

2.5 Ferroelectric nematic phase (N_F): Twisted structure

The interesting feature involves observing unusual textures in the N_F phase in a 4 µm cell shown in Figure 11, marked A-G. The angle between the analyzer (A) and the polarizer (P)is varied in this experiment.

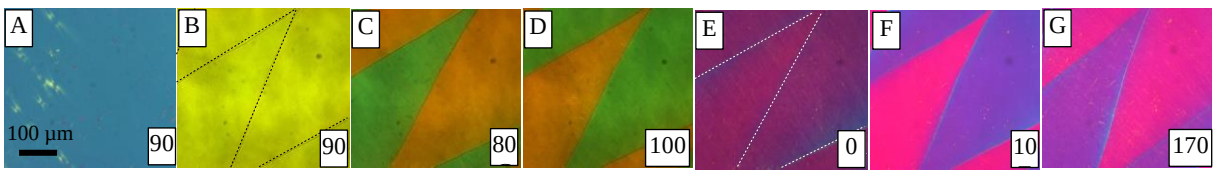

FIG. 11 The POM textures from 4 μm cell with unidirectional antiparallel rubbing of substrates at a temperature of 61 ^{o}C in the N_F phase. The homogeneous texture A transforms to the twisted texture B. The textures C to G are recorded for different angles between the *P* and *A*, the angles are shown in the righthand bottom corner of Figures 11A to 11G.

The homogeneous texture A is observed close to the N_X-N_F transition temperature transforms to the twisted texture B as temperature within the N_F phase is reduced by 2.5 ^{o}C below the N_X-N_F phase transition temperature, the 'yellow texture B' does not show the extinction of light between the crossed polarizers (Fig. 11B), the texture from parallel polarizers (Fig. 11E) appears as uniform/monodomains. The rotation of the analyzer by angles of ± 10° from the crossed positions are shown (C/D) and rotations by ± 10° from the parallel positions of **P** and **A** are marked (F/G). These textures show two domains in which their colors are swapped by the opposite rotations of the analyzer from the crossed polarizers position. The twist angle between the directors from the top to the bottom of the cell is dependent on a competition between the two energy terms in Eq. (5) of reference [14]. The twist angle would exactly be 180° only in the case of a negligibly small elastic constant. In order to examine these textures quantitively, we simulate color of the transmittance spectra for different angles between the P and A using the conventional Berreman's 4 x 4 matrix method [23]. The best simulation results are achieved for planar twisted structure where the director uniformly rotates from the top to the bottom substrate of the cell by ± 170°. for anti-parallel rubbed substrates. In a realistic elastic medium, the twist angle is dependent on the term $Kd/\omega W_Q$ and it may vary from 0° ($Kd/\omega W_Q \rightarrow \infty$) to 180° ($Kd/\omega W_Q \rightarrow 0$). However, in our experimental conditions, the twist angle is found as ~170°. The result is of higher precision than found previously by the observation of the orientation of the disclination lines under polarized microscopy [25]. Figure 12 presents the simulated optical spectra of the textures corresponding to Figs. 11A to 11G. The colors of the simulated spectra with the twist of the directors between the top and bottom substrates for different angles between **P** and **A** agree completely with the observed optical texture. The twisted structure of the nematic directors is confirmed in the N_F phase. Similar domains as those observed here for DIO were seen in the other N_F compound RM734, and their director structures were found as twisted [24,25,26].

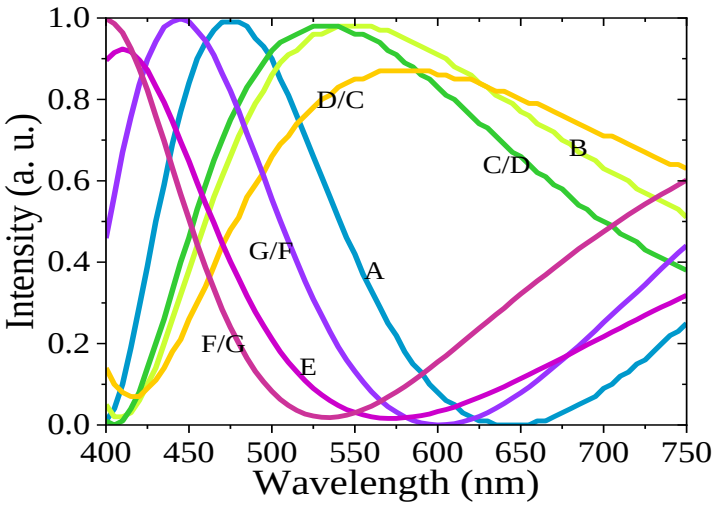

FIG. 12. Simulated optical spectra corresponding to the textures A-G shown in Fig. 7.

It is to be noted that the twisted state is achieved in the cells with antiparallel rubbing on the two opposite surfaces, while for a similar cell of the same thickness but with parallel rubbing of the alignment layers, the texture stays homogeneously planar in the entire temperature range. This phenomenon is explained by the large polar azimuthal anchoring surface energy, suggested by the Boulder group [25]. This polar in-plane anisotropy stabilizes the homogeneous planar structure for the parallel rubbing and gives twisted structure for the antiparallel rubbing.

3. Conclusion

The compound DIO with non-chiral molecules exhibits three nematic subphases. Our texture and the EO studies of this material confirm the phase sequence. However, some of these phases reveal several additional important features not reported before. N is like an ordinary nematic phase with a conventional $\Delta n(T)$ dependence in planar-aligned cells on temperature. But it also shows chiral domains of the opposite chirality under certain conditions. This is the first example of the helical segregation having occurred of non-chiral molecules; the segregated molecules form chiral domains. The other unusual feature (related to chirality) is the polarity which is responsible for the observation of the electrooptic EO response to the fundamental frequency (linear response) as opposed to the second harmonic response in a conventional nematic phase. The ferroelectric nematic N_F exhibits a strong polar azimuthal surface interaction energy [25] which stabilizes the homogeneous structure in a planar aligned cell rubbed parallel and forms the twisted

structures in the cell rubbed antiparallel. Simulation of the spectra shows that the directors are twisted by ~170° between the top and the bottom antiparallel rubbed substrates as opposed to 180° observed previously.

Acknowledgement

One of the authors NY thanks the Irish Research Council for awarding the Government of Ireland PDF 2021, GOIPD/2021/858; WJ thanks the CSC, China for a PhD scholarship.

References:

[1] M. Born, Über anisotrope Flüssigkeiten. Versuch einer Theorie der flüssigen Kristalle und des elektrischen Kerr-Effekts in Flüssigkeiten. Sitzungsber. Preuss. Akad Wiss. **30**, 614 (1916).

[2] R. J. Mandle, S. J. Cowling, and J. W. Goodby, Rational design of rod-like liquid crystals exhibiting two nematic phases. Chem. Eur. J. **23**, 14554 (2017).

[3] H. Nishikawa *et al*, A fluid liquid crystal material with highly polar order. Adv. Mater. **29**, 1702354 (2017)

[4] Y. Song, J. Li, R. Xia, H. Xu, X. Zhang, H. Lei, W. Peng, S. Dai, S. Aya and M. Huang, Development of emergent ferroelectric nematic liquid crystals with highly fluorinated and rigid mesogens. Phys. Chem. Chem. Phys. **24**, 11536 (2022).

[5] X. Chen, E. Korblova, D. Dong *et al*., First-principles experimental demonstration of ferroelectricity in a thermotropic nematic liquid crystal: polar domains and striking electro-optics. Proc. Natl. Acad. Sci. U.S.A. **117**, 14021 (2020).

[6] O. D. Lavrentovich, Proc. Natl. Acad. Sci. U.S.A. **117**,14629 (2020).

[7] N. V. Madhusudana, Simple molecular model for ferroelectric nematic liquid crystals exhibited by small rodlike mesogens. Phys. Rev. E **104**, 014704 (2021)

[8] M.P. Rosseto and J.V. Selinger, Theory of the splay nematic phase: Single versus double splay. Phys. Rev. E **101**, 052707 (2020).

[9] E.I. Kats, Stability of the uniform ferroelectric nematic phase. Phys. Rev. E **103**, 012704 (2021).

[10] A. V. Emelyanenko, V. Yu. Rudyak, S. A. Shvetsov, F. Araoka, H. Nishikawa and K. Ishikawa, Emergence of paraelectric, improper antiferroelectric, and proper ferroelectric nematic phases in a liquid crystal composed of polar molecules. Phys. Rev. E **105**, 064701 (2022).

[11] X. Chen, V. Martinez, E. Korblova, *et al*., Antiferroelectric Smectic Ordering as a Prelude to the Ferroelectric Nematic: Introducing the Smectic Z_A Phase. arXiv:2112.14222 [cond-mat. soft] (2021).

[12] F. Caimi, G. Nava, R. Barboza, N. A. Clark, E. Korblova, D. M. Walba, T. Bellini, and L. Lucchetti, Surface alignment of ferroelectric nematic liquid crystals. Soft Matter **17**, 8130 (2021).

[13] S. Brown, E. Cruickshank, J.M.D. Storey, C.T. Imrie, D. Pociecha, M. Majewska, A. Makal and E. Gorecka, Multiple polar and non-polar nematic phases. ChemPhysChem. 22, 2506 (2021).

[14] B. Basnet, M. Rajabi, H. Wang, P. Kumari, K. Thapa, S. Paul, M. O. Lavrentovich and O.D. Lavrentovich, Nature Comms,**13**,3932 (2022).

[15] T. Niori, T. Sekine, J. Watanabe, T. Furukawa, and H. Takezoe, Distinct ferroelectric smectic liquid crystals consisting of banana shaped achiral molecules. J. Mater. Chem., **6**, 1231 (1996).

[16] S. P. Sreenilayam, Y. P. Panarin, J. K. Vij, V. P. Panov, A. Lehmann, M. Poppe, M. Prehm and C. Tschierske, Spontaneous helix formation in non-chiral bent-core liquid crystals with fast linear electro-optic effect. Nat. Commun.**7**, 11369 (2016).

[17] V. P. Panov, M. Nagaraj, J. K. Vij, Y. P. Panarin, A. Kohlmeier, M. G. Tamba, R. A. Lewis, and G. H. Mehl, Spontaneous Periodic Deformations in Nonchiral Planar-Aligned Bimesogens with a Nematic-Nematic Transition and a Negative Elastic Constant. Phys. Rev. Lett.,**105**,167801 (2010).

[18] V. P. Panov, R. Balachandran, M. Nagaraj, J. K. Vij, M. G. Tamba, A. Kohlmeier, and G. H. Mehl, Microsecond linear optical response in the unusual nematic phase of achiral bimesogens. Appl. Phys. Lett. **99**, 261903 (2011).

[19] C. Dressel, T. Reppe, M. Prehm, M. Brautzsch, and C. Tschierske, Chiral self-sorting and amplification in isotropic liquids of achiral molecules. Nature Chem. **6**, 971 (2014).

[20] S. Toxvaerd, Molecular Dynamics Simulations of Isomerization Kinetics in Condensed Fluids. Phys. Rev. Lett. **85**, 4747 (2000).

[21] S. Sreenilayam, N. Yadav, Y.P. Panarin, J. K. Vij, and G. S. Shanker, Electrooptic, pyroelectric and dielectric spectroscopic studies of nematic and twist bend nematic phases of achiral hockey-shaped bent-core liquid crystal. J. Mol. Liq. **351**, 118632 (2022).

[22] I. Haller, Thermodynamic and static properties of liquid crystals, Prog. Solid State Chem. **10**, 103–118 (1975), https://doi.org/10.1016/0079-6786 (75) 90008-4.

[23] D. W. Berreman, Optics in Stratified and Anisotropic Media: 4×4-Matrix Formulation. J. Opt. Soc. Am. **62**, 502 (1972)

[24] N. Sebastián, R. J. Mandle, A. Petelin, A. Eremin, and A. Mertelj, Electrooptics of mm-scale polar domains in the ferroelectric nematic phase. Liq. Cryst. **48**, 2055 (2021). DOI: 10.1080/02678292.2021.1955417

[25] X. Chen, E. Korblova, M. A. Glaser, J. E. Maclennan, D. M. Walba, and N. A. Clark, Polar in-plane surface orientation of a ferroelectric nematic liquid crystal: Polar monodomains and twisted state electro-optics. Proc. Natl. Acad. Sci. U.S.A. **118**, e2104092118 (2021)

[26] P. Rudquist, Revealing the polar nature of a ferroelectric nematic by means of circular alignment. Sci. Reports **11**, 24411 (2021).